Dalton Transactions

Accepted Manuscript

This article can be cited before page numbers have been issued, to do this please use: N. A. Carmos dos Santos, M. Natali, E. Badetti, K. Wurst, G. Licini and C. ZONTA, *Dalton Trans.*, 2017, DOI: 10.1039/C7DT02666H.

ROYAL SOCIETY OF CHEMISTRY

rsc.li/dalton

View Article Online
DOI: 10.1039/C7DT02666H

Journal Name

ARTICLE

Cobalt, nickel, and iron complexes of 8-hydroxyquinoline-di(2-picolyl)amine for light-driven hydrogen evolution

Received 00th January 20xx,
Accepted 00th January 20xx

DOI: 10.1039/x0xx00000x

www.rsc.org/

Nadia Alessandra Carmo dos Santos,[a] Mirco Natali,*[b] Elena Badetti,[a] Klaus Wurst,[c] Giulia Licini[a] and Cristiano Zonta*[a]

Novel cobalt, nickel, and iron complexes based on the pentadentate 8-hydroxyquinoline-di(2-picolyl)amine ligand have been synthesized and thoroughly characterized. X-ray structures of both the cobalt and iron complexes have been also obtained showing the tendency to adopt a pseudo-octahedral geometry by coordination of an additional sixth ligand. The series of metal complexes have been then studied as potential hydrogen evolving catalysts (HECs) under both electrochemical and light-driven conditions. In particular, two different photochemical systems have been tested involving either the $Ru(bpy)_3^{2+}$/ascorbic acid or the $Ir(ppy)_2(bpy)^+$/TEA sensitizer/sacrificial donor couples. The electrochemical results show that these metal complexes may behave as competent HECs. However, under photochemical conditions, only the cobalt compound display substantial hydrogen evolving activity in both ruthenium- and iridium-based systems. The nickel and iron complexes, on the other hand, exhibit appreciable photocatalytic activity only in the iridium-based photochemical system, while showing negligible hydrogen evolution ability when employed in the ruthenium-based one.

Introduction

One major issue that human society has to address in the current century is the identification of renewable energy sources that are abundant, widespread, and cheap.[1] Solar-driven water splitting, with production of hydrogen gas as a clean fuel, represents a viable solution, although posing as a major challenge.[2] Huge efforts have been indeed dedicated in the last years toward the preparation and characterization of molecular hydrogen evolving catalysts (HECs),[3] with particular emphasis on their implementation into light-driven photoreaction schemes.[4] Special attention in this research field has been mainly paid toward the investigation of HECs based on first-row transition metals,[5,6,7,8] being cheaper, more abundant, and less toxic with respect to noble-metals, and thus compatible with a sustainable energy approach.[3c] Among the HECs studied, metal complexes based on polypyridine ligands have received substantial consideration,[9] since they combine several key features such as synthetic ease and flexibility, efficient catalytic activity particularly in purely aqueous solutions, and enhanced stability under turnover conditions. Due to our recent interest in the molecular recognition and catalytic properties of these systems[9l,10,11] we decided to move our attention toward the synthesis and characterization of four metal complexes **3a-d** obtained by coordination of the new pentadentate ligand **2**, the 8-hydroxyquinoline-di(2-picolyl)amine, with first-row transition metals such as cobalt, nickel, iron, and zinc (Scheme 1).

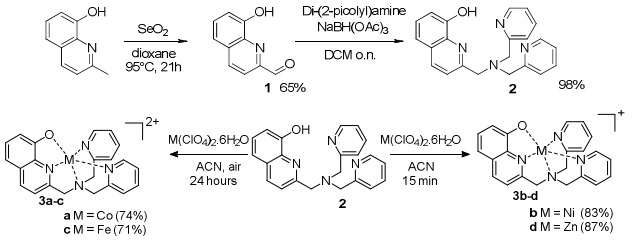

Scheme 1. General synthetic procedure for the preparation of ligand **2** and metal complexes **3a-d**.

Once assessed their potential ability to act as competent HECs, the new complexes have been tested under photoactivated conditions within two different photochemical systems, namely (i) an aqueous solution (1 M acetate buffer, pH 5) with $Ru(bpy)_3Cl_2{\cdot}6H_2O$ (where bpy = 2,2'-bipyridine) as the sensitizer and ascorbic acid as the sacrificial electron donor and (ii) a 50/50 acetonitrile/water mixture (pH 10) using $Ir(ppy)_2(bpy)PF_6$ (where ppy = 2-phenylpyridine and bpy = 2,2'-bipyridine) as the chromophore and triethylamine (TEA) as the sacrificial reagent. Positive and negative aspects of the new complexes studied in relation to *state-of-the-art* polypyridine

[a] Department of Chemical Sciences, University of Padova, Via F. Marzolo 1, 35131 Padova, Italy. E-mail: cristiano.zonta@unipd.it
[b] Department of Chemical and Pharmaceutical Sciences, University of Ferrara, and Centro Interuniversitario per la Conversione Chimica dell'Energia Solare (SolarChem), sez. di Ferrara, via L. Borsari 46, 44121 Ferrara, Italy. E-mail: mirco.natali@unife.it
[c] Institute of General, Inorganic and Theoretical Chemistry, University of Innsbruck, A-6020 Innsbruck, Austria.

Electronic Supplementary Information (ESI) available: detailed synthetic procedure for the preparation of $Ir(ppy)_2(bpy)PF_6$, characterization of ligand **2** and complexes **3a-d**, relevant crystallographic data of complexes **3a,c**, electrochemistry of complexes **3a-d**, comparison of absorption spectra before/after photocatalysis. See DOI: 10.1039/x0xx00000x

View Article Online
DOI: 10.1039/C7DT02666H

metal complexes used in photocatalytic hydrogen evolving reaction (HER) schemes will be discussed.

Results and discussion

Synthesis and Coordination Chemistry

Ligand **2** has been prepared in two steps by oxidation of commercially available 2-methyl-8-quinolinol with selenium dioxide in dioxane for 21 hour at 95°C to give 8-hydroxyquinoline-2-carboxaldehyde,[12] followed by reductive amination with di(2-picolyl)amine (Scheme 1, top). The compound is a light yellow oil and can be obtained in good yield. The general procedure for the synthesis of the metal complexes requires the mixing of an equimolar amount of ligand **2** to the corresponding dicationic perchlorate salt (Co^{2+}, Ni^{2+}, Fe^{2+}, or Zn^{2+}) in acetonitrile. The solution was stirred at room temperature (15 minutes for the nickel and zinc cases, 24 hours for both cobalt and iron) and the desired compounds were obtained either as crystalline powders or by recrystallization with diethyl ether (Scheme 1, bottom). While in the case of the nickel and zinc metal centres the complexes are stable in their original oxidation state (i.e., +2), in the case of cobalt and iron the crystallisation process in air leads to the formation of the cobalt(III) and iron(III) complexes (see below). The obtained products have been characterized by ESI-MS and Elemental Analysis (see ESI). In the case of complexes **3a** and **3c** it was also possible to obtain crystals suitable for X-ray diffraction. The molecular structure of both complexes are displayed in Figure 1, while relevant crystallographic data are reported in Table S1. In the crystal structure of complex **3a** (Figure 1, top; relevant bond lengths and angles are gathered in Table S2 and S3, respectively), the central cobalt ion is observed to be six-coordinated with a distorted octahedral geometry wherein the pentadentate 8-hydroxyquinoline-di(2-picolyl)amine ligand is shown to chelate the metal centre and an acetonitrile solvent molecule is placed in the apical position to complete the pseudo-octahedral coordination motif. The distortion with respect to the ideal octahedral geometry is expected to be largely imparted by the structural constrain of the chelating ligand, as demonstrated by the bond angles between the cobalt centre and the nitrogen atoms which result systematically lower than 90° (see Table S3). Importantly, the average Co-N bond length is 1.907(4) Å and falls within the range typically observed for related cobalt(III) polypyridine complexes,[13] thus confirming the occurrence of a Co(II)-to-Co(III) oxidation during the crystallization process under air-equilibrated conditions.¥ Interestingly, the shortest length is observed for the Co-N(2) bond (1.734 Å, see Table S2) which might be related to both the better σ-donation and π-back-bonding abilities of the quinoline moiety with respect to the amine and pyridine ligands.[14] These enhanced electronic effects exerted by the quinoline moiety on the cobalt centre are also seen to remarkably influence the length of the bond between the metal and the acetonitrile solvent molecule, resulting in the elongation of the Co-N bond (2.012 Å, see Table S2) with respect to the average distance. Importantly, this latter observation may be potentially relevant in order to enable those processes (namely ligand detachment and proton coordination) which are typically expected in the catalytic HER mechanism by a six-coordinated metal complex.[5,9]

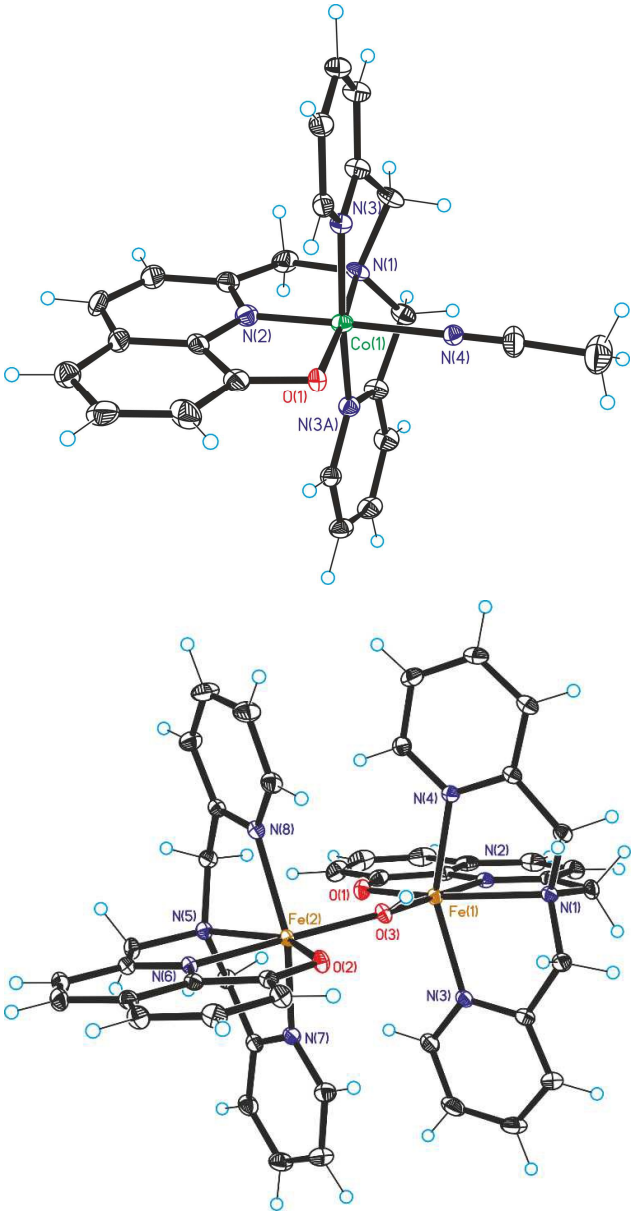

Fig. 1. Crystal structure of complexes **3a** (top) and **3c** (bottom) with selected atom labeling.

Interestingly, in the case of the iron analogue **3c**, the crystallization process leads to the formation of a dinuclear structure as determined by X-ray diffraction (Figure 1, bottom; relevant bond lengths and angles are collected in Table S4 and S5 of the ESI, respectively). Both iron centres are surrounded by one 8-hydroxyquinoline-di(2-picolyl)amine ligand and a hydroxo group *trans* to the quinolinic nitrogen, with the latter acting as a bridging ligand and completing a six-coordinating environment around the metal centres in a distorted pseudo-

View Article Online
DOI: 10.1039/C7DT02666H

octahedral geometry. The two hydroxyquinoline moieties are oriented toward opposite directions and lie within the same plane of the Fe-O(H)-Fe bridge. Similarly to the cobalt case, the observed distortion appears largely determined by the structural constrain exerted by the chelating pentadentate ligand. The two iron complexes within the dimeric species are similar in terms of coordination motif and geometry, although they are not completely identical since slightly different bond distances and angles are measured (Table S4 and S5), likely attributable to different intramolecular interactions in the solid state.[15] More importantly, the average Fe-N bond length (2.147 Å, see Table S4) and the mean Fe-O distance (1.944 Å) are comparable to those found for related iron(III) complexes featuring a similar ligand environment[15,16] and thus confirm the presence of a 3+ metal centre. Also, the Fe(1)···Fe(2) distance (3.710 Å, see Table S4) and the Fe(1)-O(3)-Fe(2) bond angle (142.07°, see Table S5) fall within the range typically observed for unsupported μ-OH-bridged Fe(III) dimers featuring similar coordination motifs.[15] While showing up as a dinuclear species in the solid state, complex **3c** appears as a monomeric compound in fluid solution, as demonstrated by ESI-MS analysis. In fact, this is not unexpected in view of the potential liability of the hydroxo bridge in a strongly coordinating environment.

Electrochemical Studies

Electrochemical measurements were performed in acetonitrile solutions (0.1 M $TBAPF_6$) in order to obtain information on the redox properties of the **3a-c** complexes. Complex **3d** was also studied and used as a reference compound for the straightforward attribution of the metal-based redox events. All the potentials are gathered in Table 1. Upon cathodic scan, complex **3a** (Figure S1) shows an irreversible process with a cathodic peak at E = −0.17 V vs. SCE, which is attributable to a Co(III)/Co(II) reduction. The irreversibility is clearly observable from the absence of the anodic peak in the return scan (at least in the potential window examined) and can be attributed either to the expected structural rearrangement occurring upon reduction from low-spin Co(III) to high-spin Co(II), as already observed for related cobalt complexes,[9b] or to the detachment of a ligand from the cobalt centre, most likely involving the coordinated solvent molecule.[17,18] At more negative potential, a reversible redox process is also observed with an $E_{1/2}$ = −1.62 V vs. SCE, which is attributable to a Co(II)/Co(I) reduction step. In the potential window investigated, complex **3b** (Figure S2) shows only a quasi-reversible redox process at an $E_{1/2}$ = −1.44 V vs. SCE, that is ascribable to a Ni(II)/Ni(I) reduction. A poorly intense anodic peak is also observed at ca E = −0.8 V vs. SCE upon subsequent scans, likely associated to some adsorption phenomena occurring at highly cathodic potentials.

Complex **3c** exhibits a redox process with an $E_{1/2}$ = −0.01 V vs. SCE (Figure S3) that is compatible with a reversible Fe(III)/Fe(II) interconversion, while at more negative potentials a not-perfectly reversible redox process is observed with a peak potential of E = −1.79 V vs. SCE, possibly attributable to an additional metal-based Fe(II)/Fe(I) reduction.

Finally, in the investigated potential range, the zinc complex **3d** displays an irreversible cathodic process with a peak potential of E = −1.97 V vs. SCE (Figure S4), which can be assigned to reduction of the coordinated 8-hydroxyquinoline-di(2-picolyl)amine ligand, thus confirming the attributions of the metal-based redox processes previously made with complexes **3a-c**.§

Table 1. Electrochemical data of complexes **3a-d**.[a]

Complex	E [M(III)/M(II)], V	E [M(II)/M(I)], V	E [L/L$^-$], V [b]
3a	−0.17 [c,d]	−1.62	-
3b	-	−1.44	-
3c	−0.01	−1.79 [c,d]	-
3d	-	-	−1.97 [c,d]

[a] Obtained by cyclic voltammetry on 1 mM **3a-d** solutions in acetonitrile (0.1 M $TBAPF_6$) at r.t., scan rate v = 100 mV/s, potentials given vs. SCE reference electrode; [b] L is the coordinated ligand **2**; [c] irreversible wave; [d] cathodic peak potential given.

Cyclic voltammetry experiments on the three redox active metal complexes **3a-c** were then performed upon addition of several aliquots of acetic acid, in order to preliminarily assess their potential ability to act as competent hydrogen evolving catalysts (HECs) under light-activated conditions.

Addition of acetic acid to an acetonitrile solution containing complex **3a** (Figure 2a) triggers the appearance of intense waves with an onset at ca E = −1.3 V vs. SCE, which increase in intensity with increasing acid concentration and can be ascribed to catalytic hydrogen evolution promoted by the cobalt centre.[18,19] The observed behaviour (onset potential at E > E[Co(II)/Co(I)], constant onset potential with increasing acid concentration) is similar to those observed with related cobalt(II) polypyridine complexes.[9b,g,l] Accordingly, a similar mechanism can be envisioned for proton reduction to dihydrogen involving Co(II)/Co(I) reduction and protonation, to yield a Co(III)-H intermediate, with the latter undergoing a subsequent reduction to a Co(II)-H species prior to hydrogen evolution.[18,20]

In the case of complex **3b** (Figure 2b), upon addition of increasing aliquots of acetic acid the Ni(II)/Ni(I) reduction process shifts progressively toward less negative potentials and becomes also irreversible, while maintaining comparable cathodic peak current values. Current enhancement is then observed with an onset at ca E = −1.5 V vs. SCE featuring acid-dependent intensity, thus attributable to catalytic proton reduction to dihydrogen. The positive shift of the Ni(II)/Ni(I) process is consistent with the occurrence of a proton-coupled electron-transfer step involving formation of a Ni(III)-H intermediate.[21,22] However, the observation that the catalytic wave starts at more negative potentials than the Ni(II)/Ni(III)-H PCET process is consistent with the requirement of an additional Ni(III)-H/Ni(II)-H reduction step which, contrarily to the related process in the cobalt case (see above), happens to be more difficult (i.e., thermodynamically more demanding) than the first electron transfer.[23] Subsequent protonation or coupling between two M(II)-hydride species, as in the case of complex **3a**, are then expected to promote hydrogen release.[24]

View Article Online
DOI: 10.1039/C7DT02666H

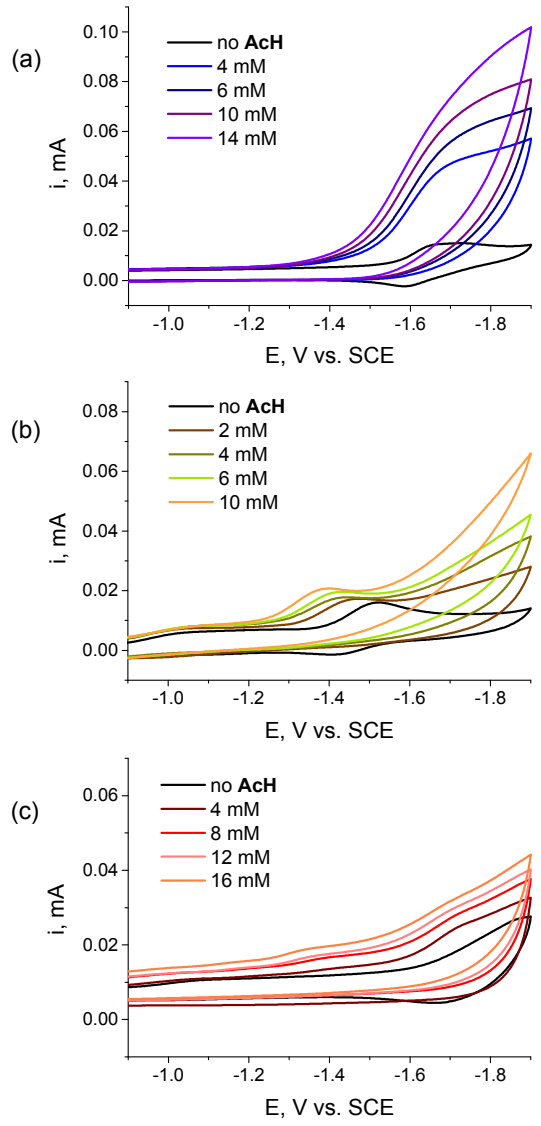

Fig. 2. Cyclic voltammetry of (a) 1 mM **3a**, (b) 1 mM **3b**, and (c) 1 mM **3c** in acetonitrile solution (0.1 M $TBAPF_6$) upon addition of several aliquots of acetic acid (**AcH**). Experimental conditions: GC as WE, Pt as CE, SCE as reference, scan rate v = 100 mV/s.

The electrochemical profile of complex **3c** changes as well upon addition of several aliquots of acetic acid (Figure 2c) with a current enhancement observed at E < −1.5 V vs. SCE which is dependent on acid concentration and thus compatible with catalytic proton reduction by the iron complex. The onset is more positive than the Fe(II)/Fe(I) reduction process, suggesting that proton reduction proceeds upon Fe(II)-to-Fe(I) reduction and protonation,[8] most likely followed, similarly to **3a,b**, by an additional reduction step prior to hydrogen elimination.[18,20] §§ For all complexes **3a-c**, hydrogen formation was detected in controlled potential electrolysis experiments (1 mM **3a-c**, 0.1 M $TBAPF_6$ acetonitrile solution, 20 mM acetic acid, constant potential of −1.7 V and −1.8 V vs. SCE for **3a,c** and **3b**, respectively) thus confirming the attribution of the observed current enhancement in the CV experiments to electrocatalytic hydrogen generation. However, low faradaic efficiencies (FE) were found in all cases (~30 % for **3a**, ~20 % for **3b**, and ~15 % for **3c** after one hour electrolysis), possibly attributable to concomitant, competitive catalyst degradation and deactivation.[26] In summary, the electrochemical studies show that among the **3a-c** series, all complexes may behave as competent HECs, although the potentials required to power hydrogen evolution appear substantially negative in all cases. As a matter of fact, a comparison of the onset potentials of the catalytic wave with respect to those of other polypyridine metal complexes recently reported[8e,f,9b,h] shows that all the complexes **3a-c** always display more negative onset potentials for the HER than typically observed. For instance, in the case of **3a**, a difference by ca 200 mV is seen under comparable experimental conditions (acetonitrile solution, acetic acid as the proton source) with respect to a related pentapyridine cobalt complex.[9b] The reason for this substantial shift can be very likely ascribed to the electron donating effect of the hydroxyquinoline fragment which enhances the electronic density on the metal centre thus moving the metal-based reduction events toward more negative potentials.

Photocatalytic Hydrogen Evolution

The potential ability of complexes **3a-c** to act as HECs was then assessed in light-driven experiments which are of fundamental importance toward the identification of suitable sensitizer/catalyst couples to be exploited in artificial photosynthetic schemes. These experiments are typically accomplished in aqueous solutions or organic/aqueous mixtures combining three molecular components, namely a HEC, a photosensitizer (P), and a sacrificial electron donor (D).[2e,4c,5c] The inactive zinc complex **3d** was tested as well, in order to provide a suitable blank experiment for the sake of comparison. Complexes **3a-d** were tested under two different photoreaction conditions: (i) in a purely aqueous solution (1 M acetate buffer, pH 5) in combination with $Ru(bpy)_3^{2+}$ as the sensitizer (P) and ascorbic acid as the sacrificial electron donor (D) and (ii) in a 50/50 acetonitrile/water mixture (pH 10) using $Ir(ppy)_2(bpy)^+$ as the chromophore (P) and triethylamine as the sacrificial agent (D). According to literature precedents on both the ruthenium-[5f,9,27] and iridium-based[28,29] systems, photoinduced hydrogen evolution by a suitable HEC (eq 6) is expected to occur after the following (photo)chemical steps (protonation steps are herein neglected for simplicity reasons): light absorption (eq 1), reductive quenching of the excited chromophore by the sacrificial electron donor (eq 2) with the latter undergoing irreversible transformation upon oxidation (eq 3), two consecutive one-electron transfers to the HEC from the photogenerated reduced sensitizer (eqs 4,5).‡

$$P + h\nu \rightarrow {}^*P \quad (1)$$
$${}^*P + D \rightarrow P^- + D^+ \quad (2)$$
$$D^+ \rightarrow \text{products} \quad (3)$$
$$P^- + HEC \rightarrow P + HEC^- \quad (4)$$
$$P^- + HEC^- \rightarrow P + HEC^{2-} \quad (5)$$
$$HEC^{2-} + 2H^+ \rightarrow HEC^{2-} + H_2 \quad (6)$$

View Article Online
DOI: 10.1039/C7DT02666H

Apart from effects on photocatalysis arising from the different environments used (presence of an organic co-solvent, solution pH, etc.)[30] and the different absorption properties of the two sensitizers throughout the visible spectrum (where irradiation is performed, see Figure S7), the $Ru(bpy)_3^{2+}$/ascorbic acid and the $Ir(ppy)_2(bpy)^+$/TEA systems differ substantially in that the reducing agents that are photogenerated via reductive quenching by the donor (eq 2) have different redox potentials, resulting in different thermodynamics for the HEC activation steps (eqs 4,5). Indeed, the reduced ruthenium dye has a reduction potential of E = −1.28 vs. SCE in aqueous solution,[31] while the reduced iridium chromophore has a reduction potential of E = −1.43 vs. SCE,[29] with the latter thus resulting a more powerful reducing agent by 150 mV than the former.

Photocatalytic hydrogen evolution experiments were thus performed upon visible light irradiation of solutions containing (i) **3a-d**, $Ru(bpy)_3^{2+}$, and ascorbic acid and (ii) **3a-d**, $Ir(ppy)_2(bpy)^+$, and TEA. Experimental conditions (type of buffer and concentration, solvent mixture and composition, solution pH, etc.) were taken according to previous reports on photochemical hydrogen evolution systems based on such chromophore/donor couples.[9,29] In particular, in the ruthenium-based system the concentrations of the reactants in the photolysis mixture were as follows: 0.1 mM **3a-d**, 0.5 mM $Ru(bpy)_3Cl_2{\cdot}6H_2O$, 0.1 M ascorbic acid in 1 M acetate buffer at pH 5. In the iridium-based three-component system the experimental conditions were as described herein: 0.1 mM **3a-d**, 0.5 mM $Ir(ppy)_2(bpy)PF_6$, 45/45/10 acetonitrile/water/TEA mixture at pH 10. All the kinetic traces (average of two independent experiments) are reported in Figure 3a, while relevant photocatalytic data (TONs and maximum TOFs) are collected in Figure 3b for comparison (in the latter instance the parameters are reported with respect to the amount of complex **3a-d** in solution regardless of the metal present).

The cobalt complex **3a** is active as a HEC when employed in both the ruthenium- and iridium-based photochemical systems achieving turnover number (TON) of 10 and 19 after 2 hour irradiation with maximum turnover frequency (TOF) of 7.2 and 16.2 h^{-1}, respectively (Figure 3b). The nickel and iron complexes **3b,c**, on the other hand, behave similarly, exhibiting a lower hydrogen evolution activity with only a TON = 4 and 5, respectively, after 2 hour irradiation with a maximum TOF = 3.0 and 2.4 h^{-1}, respectively, when studied in the iridium-based photochemical system (Figure 3b), while they are practically inactive (TON < 1, low TOF) when employed in the ruthenium-based one. As expected, the zinc complexes **3d** displays an almost negligible hydrogen production yield (low maximum TOF, consistent with negligible quantum efficiency for the reaction) when employed in both the ruthenium- and iridium-based photochemical systems, with the trace amounts of hydrogen detected likely arising from slow, direct reduction of protons by the photogenerated reduced sensitizer species. Interestingly, when the activity of the metal complexes **3a-c** is compared, the trend observed in terms of both TON and maximum TOF with respect to the photocatalytic system studied shows that (i) the cobalt complex **3a** is always more active than the nickel and iron complexes **3b,c**, (ii) with the same metal complex the iridium-based photochemical system is always more efficient than the ruthenium-based one. This observation can be explained, at least qualitatively, on simple thermodynamic basis considering that the cobalt complex **3a** is capable of promoting hydrogen evolution at a lower potential than the parent complexes **3b,c** (see above and Figure 2) and thus catalyst activation from the photogenerated reducing agent (eqs 4,5) is expected to be more favourable in the former case.‖

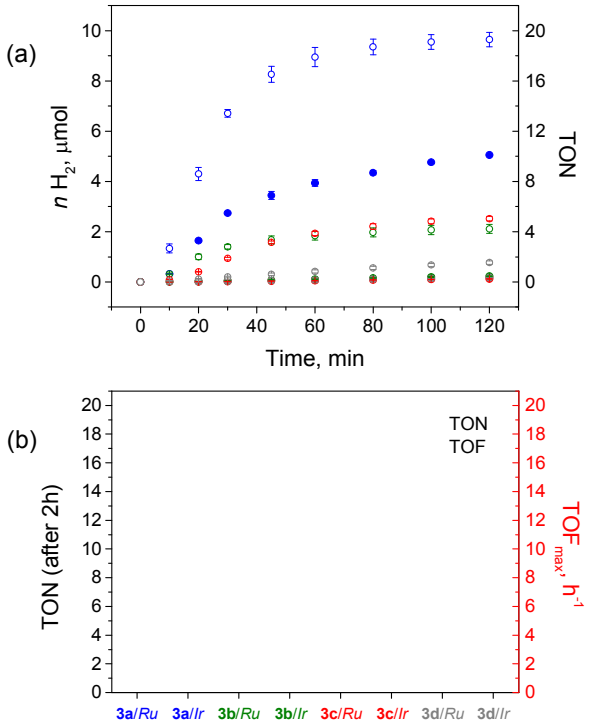

Fig. 3. (a) Photocatalytic hydrogen evolution kinetics (average of two independent experiments) using complexes **3a** (blue dots), **3b** (green dots), **3c** (red dots), and **3d** (grey dots) in the ruthenium- (full dots) and iridium-based (empty dots) photochemical systems and (b) relevant photocatalytic data. Experimental conditions: **Ru** system: 0.1 mM **3a-d**, 0.5 mM $Ru(bpy)_3Cl_2$, 0.1 M ascorbic acid in 1 M acetate buffer at pH 5; **Ir** system: 0.1 mM **3a-d**, 0.5 mM $Ir(ppy)_2(bpy)PF_6$, 45/45/10 acetonitrile/water/TEA mixture at pH 10.

Also, the use of a more powerful reductant (as it is in the case of the iridium sensitizer) turns out to be a key factor to improve the photocatalytic efficiency with the same metal complex. This latter point is exemplified by the abatement of the light-driven hydrogen evolution activity mediated by both the nickel and iron complexes **3b,c** when the iridium-based photochemical system is replaced by the ruthenium-based one, where photocatalytic parameters close to those observed with the inactive zinc complexes **3d** are recorded (Figure 3). It is worth pointing out, however, that the photocatalytic performances of the investigated metal complexes **3a-c** are

View Article Online
DOI: 10.1039/C7DT02666H

rather modest when compared to other polypyridine complexes reported in the literature, in particular as far as cobalt-based ones are concerned, which typically display TONs even up to ~10^3 and TOFs in the "min^{-1}" regime.[9] In order to find possible explanations we compared the absorption spectra before and after 2 h photolysis (Figure S8, S9, and S10 for **3a**, **3b**, and **3c**, respectively) and observed that with all **3a-c** complexes a major abatement of the absorption patterns of both the ruthenium and iridium chromophores takes place (up to ca 60% loss of the initial absorbance in the case of the ruthenium sensitizer) comparable with what observed in the blank experiments using the zinc complex **3d** (Figure S11). This thus indicates that, regardless of the metal complex present in solution, both sensitizers undergo a substantial degradation under light irradiation, which most likely proceeds via disproportionation of and/or proton attack to the reduced chromophore species.[32] This clearly means that under the experimental conditions adopted side-reactions potentially involving the photogenerated reduced sensitizers are very likely to compete favourably with the forward electron transfer pathways involving the HEC (eqs 4,5) thereby leading to enhanced dye degradation and fast, concurrent photocatalysis inactivation. The reasons for the observed behaviour can be mostly attributed to the considerably negative potentials required to trigger the HER by metal complexes **3a-c** and thus the poor driving force for the forward electron transfer processes (eqs 4,5) which may have a profound impact onto the related kinetics.

Experimental Section

Materials

Milli-Q Ultrapure water and spectroscopic grade acetonitrile (Sigma-Aldrich) were used for the photocatalysis experiments. Anhydrous acetonitrile (Alfa Aesar) was used for the electrochemical measurements. $Ru(bpy)_3Cl_2{\cdot}6H_2O$ was purchased from Sigma-Aldrich and used as received. All other reagents were purchased from commercially available suppliers and used as received.

Synthetic procedures

General procedure for synthesis of 8-hydroxyquinoline-2-carbaldehyde (1):

We adopted a reported synthetic procedure with minor modifications.[31] Commercially available 8-hydroxy-2-methyl-quinoline (25.1 mmol) was added to a suspension of selenium oxide (8.364 g, 75.4 mmol, 3 eq) in dioxane (100 ml) under N_2 atmosphere. The mixture was heated at 95 °C during 21 h. After cooling at room temperature, the mixture was filtered on celite. The filtrate was concentrated under vacuum. Purification of the resulting crude product on silica column chromatography (dichloromethane) afforded the desired product as a yellow solid. Yield: 65%. ^{1}H NMR (200 MHz, $CDCl_3$): δ (ppm) = 10.26 (s, 1H, CHO), 8.36 (d, 1H, HAr), 8.21 (s, 1H, OH), 8.09 (d, 1H, HAr), 7.67 (t, 1H, HAr), 7.48 (dd, 1H, HAr), 7.34 (dd, 1H, HAr). ^{13}C NMR (62 MHz, $CDCl_3$): δ (ppm) = 192.94, 137.72, 131.17, 118.26, 111.43. ESI-MS m/z_{calc}: 173.1 Found $[MH]^+$ m/z: 174.1.

General procedure for synthesis of 2-((bis(pyridin-2-ylmethyl)amino)methyl)quinolin-8-ol (2):

We adopted a reported synthetic procedure with minor modifications.[32] 2-dipicolylamine (0.945 mL, 5.3 mmol) and 8-hydroxyquinoline-2-carbaldehyde (1g, 5.8 mmol, 1.1 eq) were stirred in anhydrous dichloromethane (30 mL) under N_2 atmosphere. After 3 h, sodium triacetoxy borohydride (1.446 g, 6.8 mmol, 1.3 eq) was added and the mixture was stirred under N_2 atmosphere overnight at room temperature. The mixture was washed three times with saturated $NaHCO_3$ solution and the organic phase was dried over Na_2SO_4. The solvent was removed under reduced pressure and gave the pure product as a light yellow oil. Yield: 98%. ^{1}H NMR (200 MHz, CD_3CN): δ (ppm) = 8.54 (dq, 2H, HAr), 8.24 (d, 1H, HAr), 7.70 (m, 5H, HAr), 7.43 (m, 2H, HAr), 7.18 (m, 3H, HAr), 4.03 (s, 2H, CH_2), 3.93 (s, 4H, CH_2). ^{13}C NMR (62 MHz, $CDCl_3$): δ (ppm) = 160.71, 158.62, 153.88, 150.63, 137.92, 128.90, 124.74, 123.60, 118.92, 111.56, 61.72, 61.17. ESI-MS m/z_{calc}: 356.4 Found $[MH]^+$ m/z: 357.4.

General procedure for the synthesis of metal complexes 3a-d

2-((bis(pyridin-2-ylmethyl)amino)methyl)quinolin-8-ol (50 mg, 0.14 mmol) was dissolved in the minimum amount of anhydrous acetonitrile and the desired metal salt (1 eq) was added. The solution was let stirring at room temperature for 15 min and then, diethyl ether was slowly added to the mixture to obtain the desired products by crystallization. *Caution!* Perchlorate salts of metal complexes with organic ligands are potentially explosive. They should be handled in small quantities and with caution.

3a Dark brown crystal [74%]. ESI-MS m/z_{calc}: 513.0 Found $[MClO_4]^+$ m/z: 512.9

3b Ochre crystal [83%]. ESI-MS m/z_{calc}: 413.1 Found $[M]^+$ m/z: 413.1

3c Dark green crystal [71%]. ESI-MS m/z calc : 456.1 Found $[MHCOO]^+$ m/z: 456.1

3d Dark yellow solid [87%]. ^{1}H NMR (200 MHz, CD_3CN): δ (ppm) = 8.81 (d, 2H, HAr), 8.52 (d, 1H, HAr), 8.12 (dt, 2H, HAr), 7.63 (m, 9H, HAr), 4.47 (d, 4H, CH_2), 4.39 (s, 2H, CH_2).Esi-MS m/z_{calc}: 419.1 Found $[M]^+$ m/z: 419.1

Synthesis of $Ir(ppy)_2(bpy)PF_6$. The cyclometalated iridium(III) complex $Ir(ppy)_2(bpy)PF_6$ was synthesized according to slight variations on reported literature procedures.[33] A two-step protocol was adopted, involving (i) reaction of $IrCl_3{\cdot}xH_2O$ with a slight excess of ppy (where ppy = 2-phenylpyridine) to obtain the $[Ir(ppy)_2Cl]_2$ dimer and (ii) subsequent reaction of the latter with the bpy ligand (where bpy = 2,2'-bipyridine) followed by precipitation with KPF_6 (see ESI for additional details).

Crystallography. The supplementary crystallographic data were deposited as CCDC 1556115-1556116. Copies of the data

View Article Online
DOI: 10.1039/C7DT02666H

can be obtained, free of charge, at the Cambridge Crystallographic Data Centre.

Apparatus and procedures. UV-Vis absorption spectra were recorded on a Jasco V-570 UV/Vis/NIR spectrophotometer. Cyclic Voltammetry (CV) measurements were carried out with a PC-interfaced Eco Chemie Autolab/Pgstat 30 Potentiostat. A conventional three-electrode cell assembly was adopted: a saturated calomel electrode (SCE, Amel) and a platinum electrode were used as reference and counter electrodes, respectively; a glassy carbon (GC) electrode (7 mm^2 surface area) was used as the working electrode. All experiments were performed in nitrogen-purged acetonitrile solutions. The $TBAPF_6$ supporting electrolyte was dried overnight before use. The GC electrode was accurately polished with alumina slurry after every scan. Potential controlled electrolysis experiments were performed in a gas-tight custom-made electrochemical cell using a large surface area carbon foil as the working electrode, a platinum grid as the counter electrode (separated from the test solution by a frit) and a Ag/AgCl (3 M NaCl) as the reference electrode (in the text, potentials are converted to SCE for uniformity with CV experiments). The head-space of the cell was connected to the gas-chromatography (GC) apparatus described below for the determination and quantification of hydrogen. The photochemical hydrogen evolution experiments were carried out upon continuous visible light irradiation with a 175 W Xe arc-lamp (CERMAX PE175BFA) of a reactor containing the solution (a 10 mm pathlength pyrex glass cuvette with head space obtained from a round-bottom flask). A cut-off filter at $\lambda < 400$ nm and a hot mirror (IR filtering) have been used in order to provide the useful wavelength range (400-800 nm). The gas phase of the reaction vessel was analyzed on an Agilent Technologies 490 microGC equipped with a 5 Å molecular sieve column (10 m), a thermal conductivity detector, and using Ar as carrier gas. Additional details of the setup and procedures used for the hydrogen evolution experiments can be found in previous reports.[9g,l] In a typical photocatalytic experiment, samples of 5 mL were prepared in 20 mL scintillation vials in the following manner depending on the sample studied: (i) by dilution in 1 M acetate buffer (pH 5) of $Ru(bpy)_3Cl_2{\cdot}6H_2O$ (0.5 mL from a 5 mM mother solution in 1 M acetate buffer), **3a-d** (0.05 mL, from a 0.01 M mother solution in acetonitrile), and ascorbic acid (88 mg, added as solid); (ii) by adding $Ir(ppy)_2(bpy)PF_6$ (0.5 mL from a 5 mM mother solution in acetonitrile), **3a-d** (0.05 mL, from a 0.01 M mother solution in acetonitrile), triethylamine (0.5 mL), acetonitrile (1.7 mL), and water (2.25 mL) and adjusting the pH to 10 upon addition of concentrated HCl. Once prepared, the solution was put in the reactor, degassed by bubbling Ar for 20 min, and thermostated at 17°C. The cell was then irradiated and the solution continually stirred during the photolysis. The gas phase of the reaction was analyzed through microGC and the amount of hydrogen quantified.

Conclusions

New first-row transition metal complexes **3a-d** based on the 8-hydroxyquinoline-di(2-picolyl)amine ligand have been prepared and those based on redox active metal centres (**3a-c**) studied as potential hydrogen evolving catalysts under both electrochemical and light-driven conditions. In particular, two different photochemical systems have been tested involving either the $Ru(bpy)_3^{2+}$/ascorbic acid or the $Ir(ppy)_2(bpy)^+$/TEA sensitizer/sacrificial donor couples. The electrochemical results show that all redox-active metal complexes **3a-c** may actually behave as competent HECs. Under photochemical conditions, only the cobalt compound display substantial hydrogen evolving activity in both the ruthenium- and iridium-based systems achieving TONs up to 10 and 19, respectively, with maximum TOFs of 7.2 and 16.2 h^{-1}, respectively. The nickel and iron complexes, on the other hand, exhibit appreciable photocatalytic activity only in the iridium-based photochemical system, while showing negligible hydrogen evolution in the ruthenium one, similarly to what observed with the inactive zinc complex **3d**. Complexes **3a-c**, however, display considerably lower activity toward proton reduction with respect to *state-of-the-art* polypyridine metal complexes reported in the literature. Indeed, although the chelating properties of the new 8-hydroxyquinoline-di(2-picolyl)amine ligand are favourable toward the stabilization of the metal complexes in their coordination geometry also leaving a labile (and thus potentially available) coordination site to enable proton binding, the enhanced electron donating effect of the hydroxyquinoline moiety apparently increases the electronic density on the metal centre thus shifting the metal-based reduction processes toward highly negative potentials. In this respect the formation of the nucleophilic M(I) species which is required to favour protonation as well as the subsequent reduction of the M(III)-H intermediate turn out to be thermodynamically more demanding than commonly observed with other polypyridine complexes. Therefore catalyst activation by the photogenerated reducing agent, either in the ruthenium- and iridium-based photochemical systems, may actually compete unfavourably with side-reaction phenomena thereby leading to rapid abatement of the photocatalytic activity. This work, however, still outlines the relevance of carefully controlling all the stereoelectronic effects in catalyst design in order to achieve sustained and efficient hydrogen production.

Acknowledgements

Dr. Paulina Dreyse (Universidad Técnica Federico Santa María, Valparaiso, Chile) is gratefully acknowledged for providing the $Ir(ppy)_3(bpy)PF_6$ complex used. We thank Prof. Andrea Sartorel (University of Padova) for help with the bulk electrolysis experiments. Financial support from the University of Padova (PRAT CPDA CPDA153122, Progetto Attrezzature Scientifiche finalizzate alla Ricerca 2014) is gratefully acknowledged.

Notes and references

View Article Online
DOI: 10.1039/C7DT02666H

¥ It should be also noted that the average Co-N bond length observed herein is also considerably lower than that measured in the case of related polypyridine cobalt(II) complexes used as HECs.[9]

§ The failure to observe a ligand-based reduction in the case of complexes **3a-c** can be related to the fact that this redox event likely occurs at more negative potentials than experimentally investigated. On the basis of simple electrostatic considerations, metal-based reduction processes are indeed expected to cathodically shift the ligand-based redox event.

§§ Blank experiments with **3d** and no metal complex were also performed in order to rule out concomitant proton reduction of the bare GC electrode[25] (see Figure S5 and S6, respectively). These results confirm that the observed current enhancement in the presence of acid is fully related to metal-based catalysis in the case of complexes **3a,b**, while direct contribution from the bare GC electrode cannot be completely ruled out in the case of complex **3c**. Also, the appreciably negative potentials required to observe a current enhancement in the presence of acetic acid is such that the catalytic waves cannot be completely defined in all cases thus preventing any deeper mechanistic investigation of the HER mechanism. This is, however, out of the scope of the present manuscript.

‡ An alternative photochemical mechanism, namely oxidative quenching of the excited sensitizer by the HEC (and HEC^-) and subsequent hole shift from the oxidized dye to the sacrificial donor, might be in principle operative. However, based on simple thermodynamic considerations, the reducing power of the excited states, particularly in the ruthenium case, are not sufficient to favour direct HEC (and even more HEC^-) reduction, the latter processes being indeed occurring at very cathodic potentials. Also, based on kinetic considerations, the typically high donor concentration employed in the photolysis conditions is such that the reductive quenching pathway is expected to be kinetically dominating over the competitive, if any, oxidative quenching.

‖ The observation that the iridium system always gives raise to enhanced hydrogen production with respect to the ruthenium-based one seems to be consistent with the fact that environmental effects on photocatalysis seem to play a less important role.

1 (a) N. S. Lewis and D. G. Nocera, *Proc. Natl. Acad. Sci. U.S.A.*, 2006, **103**, 15729. (b) N. Armaroli and V. Balzani, *Angew. Chem., Int. Ed.*, 2007, **46**, 52. (c) J. R. McKone, D. C. Crans, C. Martin, J. Turner, A. R. Duggal and H. B. Gray, *Inorg. Chem.*, 2016, **55**, 9131.

2 (a) J. H. Alstrum-Acevedo, M. K. Brennaman and T. J. Meyer, *Inorg. Chem.*, 2005, **44**, 6802. (b) T. R. Cook, D. K. Dogutan, S. Y. Reece, Y. Surendranath, T. S. Teets and D. G. Nocera, *Chem. Rev.*, 2010, **110**, 6474. (c) D. Gust, T. A. Moore and A. L. Moore, *Faraday Disc.*, 2012, **155**, 9. (d) J. R. McKone, N. S. Lewis and H. B. Gray, *Chem. Mater.*, 2014, **26**, 407. (e) M. Natali and F. Scandola. *Supramolecular Artificial Photosynthesis*. G. Bergamini, S. Silvi (eds.), *Applied Photochemistry*, *Lecture Notes in Chemistry* **92**, DOI: 10.1007/978-3-319-31671-0_1, Springer 2016.

3 (a) V. Artero, M. Chavarot-Kerlidou and M. Fontecave, *Angew. Chem., Int. Ed.*, 2011, **50**, 7238. (b) W. T. Eckenhoff, and R. Eisenberg, *Dalton Trans.*, 2012, **41**, 13004. (c) J. R. McKone, S. C. Marinescu, B. S. Brunschwig, J. R. Winkler and H. B. Gray, *Chem. Sci.*, 2014, **5**, 865.

4 (a) Y. Halpin, M. T. Pryce, S. Rau, D. Dini and J. G. Vos, *Dalton Trans.* 2013, **42**, 16243. (b) Z. Han and R. Eisenberg, *Acc. Chem. Res.*, 2014, **47**, 2537. (c) K. Ladomenou, M. Natali, E. Iengo, G. Charalampidis, F. Scandola and A. G. Coutsolelos, *Coord. Chem. Rev.*, 2015, **304-305**, 38. (d) M. Wang, K. Han, S. Zhang and L. Sun, *Coord. Chem. Rev.*, 2015, **287**, 1.

5 (a) P. Du, K. Knowles and R. Eisenberg, *J. Am. Chem. Soc.*, 2008, **130**, 12576. (b) A. Fihri, V. Artero, M. Razavet, C. Baffert, W. Leibl and M. Fontecave, *Angew. Chem., Int. Ed.*, 2008, **47**, 564. (c) W. T. Eckenhoff, W. R. McNamara, P. Du and R. Eisenberg, *Biochim. Biophys. Acta*, 2013, **1827**, 958. (d) F. Lakadamyali and E. Reisner, *Chem. Commun.*, 2011, **47**, 1695. (e) M. Natali, R. Argazzi, C. Chiorboli, E. Iengo and F. Scandola, *Chem. Eur. J.*, 2013, **19**, 9261. (f) E. Deponti and M. Natali, *Dalton Trans.*, 2016, **45**, 9136.

6 (a) S. Losse, J. G. Vos and S. Rau, *Coord. Chem. Rev.*, 2010, **254**, 2492. (b) C. C. L. McCrory, C. Uyeda and J. C. Peters, *J. Am. Chem. Soc.*, 2012, **134**, 3164. (c) C. Gimbert-Suriñach, J. Albero, T. Stoll, J. Fortage, M.-N. Collomb, A. Deronzier, E. Palomares and A. Llobet, *J. Am. Chem. Soc.*, 2014, **136**, 7655. (d) M. Natali, A. Luisa, E. Iengo and F. Scandola, *Chem. Commun.*, 2014, **50**, 1842. (e) S. Roy, M. Bacchi, G. Berggren and V. Artero, *ChemSusChem*, 2015, **8**, 3632.

7 (a) M. L. Helm, M. P. Stewart, R. M. Bullock, M. Rakowski DuBois and D. L. DuBois, *Science*, 2011, **333**, 863. (b) M. P. McLaughlin, T. M. McCormick, R. Eisenberg and P. L. Holland, *Chem. Commun.*, 2011, **47**, 7989. (c) Z. Han, L. Shen, W. W. Brennessel, P. L. Holland and R. Eisenberg, *J. Am. Chem. Soc.*, 2013, **135**, 14659. (d) M. A. Gross, A. Reynal, J. Durrant and E. Reisner, *J. Am. Chem. Soc.*, 2014, **136**, 356. (e) A. S. Weingarten, R. V. Kazantsev, L. C. Palmer, M. McClendon, A. R. Koltonow, A. P. S. Samuel, D. J. Kiebala, M. R. Wasielewski and S. I. Stupp, *Nat. Chem.*, 2014, **6**, 964. (f) P. H. A. Kankanamalage, S. Mazumder, V. Tiwari, K. K. Kpogo, H. B. Schelegel and C. N. Verani, *Chem. Commun.*, 2016, **52**, 13357.

8 (a) C. Tard and C. J. Pickett, *Chem. Rev.*, 2009, **109**, 2245. (b) R. Lomoth and S. Ott, *Dalton Trans.*, 2009, 9952. (c) D. Streich, Y. Astuti, M. Orlandi, L. Schwartz, R. Lomoth, L. Hammarström and S. Ott, *Chem. Eur. J.*, 2010, **16**, 60; (d) S. Pullen, H. Fei, A. Orthaber, S. Cohen and S. Ott, *J. Am. Chem. Soc.*, 2013, **135**, 16997. (e) G. P. Connor, K. J. Meyer, C. S. Tribble and W. R. McNamara, *Inorg. Chem.*, 2014, **53**, 5408. (f) A. C. Cavell, C. L. Hartley, D. Liu, C. S. Tribble and W. R. McNamara, *Inorg. Chem.*, 2015, **54**, 3325. (g) C. L. Hartley, R. J. DiRisio, M. E. Screen, K. J. Mayer and W. R. McNamara, *Inorg. Chem.*, 2016, **55**, 8865.

9 (a) C.-F. Leung, S.-M. Ng, C.-C. Ko, W.-L. Man, J. Wu, L. Chen and T.-C. Lau, *Energy Environ. Sci.*, 2012, **5**, 7903. (b) M. Nippe, R. S. Khnayzer, J. A. Panetier, D. Z. Zee, B. S. Olaiya, M. Head-Gordon, C. J. Chang, F. N. Castellano and J. R. Long, *Chem. Sci.*, 2013, **4**, 3934. (c) B. Shan, T. Baine, X. A. N. Ma, X. Zhao and R. H. Schmehl, *Inorg. Chem.*, 2013, **52**, 4853. (d) C. Bachmann, M. Guttentag, B. Spingler and R. Alberto, *Inorg. Chem.*, 2013, **52**, 6055. (e) R. S. Khnayzer, V. A. Thoi, M. Nippe, A. E. King, J. W. Jurss, K. A. El Roz, J. R. Long, C. J. Chang and F. N. Castellano, *Energy Environ. Sci.*, 2014, **7**, 1477. (f) L. Tong, R. Zong and R. P. Thummel, *J. Am. Chem. Soc.*, 2014, **136**, 4881. (g) E. Deponti, A. Luisa, M. Natali, E. Iengo and F. Scandola, *Dalton Trans.*, 2014, **43**, 16345. (h) A. Call, Z. Codolá, F. Acuña-Pares and J. Lloret-Fillol, *Chem. Eur. J.*, 2014, **20**, 6171. (i) D. Z. Zee, T. Chantarojsiri, J. R. Long and C. J. Chang, *Acc. Chem. Res.*, 2015, **48**, 2027. (j) N. Queyriaux, R. T. Jane, J. Massin, V. Artero and M. Chavarot-Kerlidou, *Coord. Chem. Rev.*, 2015, **304-305**, 3. (k) W. K. C. Lo, C. E. Castillo, R. Gueret, J. Fortage, M. Rebarz, M. Sliwa, F. Thomas, C. J. McAdam, G. B. Jameson, D. A. McMorran, J. D. Crowley, M.-N. Collomb and A. G. Blackman, *Inorg. Chem.*, 2016, **55**, 4564. (l) M. Natali, E. Badetti, E. Deponti, M. Gamberoni, F. A. Scaramuzzo, A. Sartorel and C. Zonta, *Dalton Trans.*, 2016, **45**, 14764.

10 (a) F. A. Scaramuzzo, G. Licini and C. Zonta, *Chem. Eur. J.*, 2013, **19**, 16809. (b) E. Badetti, K. Wurst, G. Licini and C. Zonta, *Chem. Eur. J.*, 2016, **22**, 6515. (c) R. Berardozzi, E.

View Article Online
DOI: 10.1039/C7DT02666H

Badetti, N. A. Carmo Dos Santos, K. Wurst, G. Licini, G. Pescitelli, C. Zonta and L. Di Bari, *Chem. Comm.*, 2016, **52**, 8428. (d) F. A. Scaramuzzo, E. Badetti, G. Licini and C. Zonta, *Eur. J. Org. Chem.*, 2017, **11**, 1438. (e) C. Bravin, E. Badetti, F. A. Scaramuzzo, G. Licini and C. Zonta, *J. Am. Chem. Soc.*, 2017, **139**, 6456–6460. (f) N. A. Carmo dos Santos, E. Badetti, G. Licini, S. Abbate, G. Longhi and C. Zonta, *Chirality*, 2017, in press.

11 N. A. Carmo dos Santos, F. Lorandi, E. Badetti, K. Wurst, A. A. Isse, A. Gennaro, G. Licini and C. Zonta *Polymer*, 2017, **128**, 169.

12 G. Tallec, D. Imbert, P. H. Friesa and M. Mazzanti, *Dalton Trans.*, 2010, **39**, 9490.

13 (a) E. C. Niederhoffer, A. E. Martell, P. Rudolf and A. Clearfield, *Inorg. Chem.*, 1982, **21**, 3734. (b) S. Ghosh, A. C. Barve, A. A. Kumbhar, A. S. Kumbhar, V. G. Puranik, P. A. Datar, U. B. Sonawane and R. R. Joshi, *J. Inorg. Biochem.*, 2006, **100**, 331.

14 A. Albert and J. N. Phillips, *J. Chem. Soc.*, 1956, 1294.

15 (a) J. Jullien, G. Juhasz, P. Mialane, E. Dumas, C. R. Mayer, J. Marrot, E. Rivière, E. L. Bominaar, E. Münck and F. Sécheresse, *Inorg. Chem.*, 2006, **45**, 6922. (b) R. Shakya, D. R. Powell and R. P. Houser, *Eur. J. Inorg. Chem*., 2009, 5319.

16 J. P. López, F. W. Heinemann, R. Prakash, B. A. Hess, O. Horner, C. Jeandey, J.-L. Oddou, J.-M. Latour and A. Grohmann, *Chem. Eur. J.*, 2002, **8**, 5709.

17 A. Panagiotopoulos, K. Ladomenou, D. Sun, V. Artero and A. G. Coutsolelos, *Dalton Trans.*, 2016, **45**, 6732.

18 E. S. Rountree, D. J. Martin, B. D. McCarthy and J. L. Dempsey, *ACS Catal.*, 2016, **6**, 3326.

19 (a) J.-M. Savéant and K. B. Su, *J. Electroanal. Chem.*, 1984, **171**, 341. (b) J.-M. Savéant, *Chem. Rev.*, 2008, **108**, 2348.

20 J. T. Muckerman and E. Fujita, *Chem. Commun.*, 2011, **47**, 12456.

21 N. Elgrishi, D. A. Kurtz and J. L. Dempsey, *J. Am. Chem. Soc.*, 2017, **139**, 239.

22 M.-H. Hu, R. Rousseau, J. A. S. Roberts, E. S. Wiedner, M. Dupuis, D. L. DuBois, R. M. Bullock and S. Raugei, *ACS Catal.*, 2015, **5**, 5436.

23 C. Costentin and J.-M. Savéant, *ChemElectroChem*, 2014, **1**, 1226.

24 J. L. Dempsey, B. S. Brunschwig, J. R. Winkler and H. B. Gray, *Acc. Chem. Res.*, 2009, **42**, 1995.

25 B. D. McCarthy, D. Martin, E. S. Rountree, A. C. Ullman and J. L. Dempsey, *Inorg. Chem.*, 2014, **53**, 8350.

26 X. Hu, B. S. Brunschwig and J. Peters, *J. Am. Chem. Soc.*, 2007, **129**, 8988.

27 G. M. Brown, B. S. Brunschwig, C. Creutz, J. F. Endicott and N. Sutin, *J. Am. Chem. Soc.*, 1979, **101**, 1298.

28 (a) J. I. Goldsmith, W. R. Hudson, M. S. Lowry, T. H. Anderson and S. Bernhard, *J. Am. Chem. Soc.*, 2005, **127**, 7502. (b) L. L. Tinker, N. D. McDaniel, P. N. Curtin, C. K. Smith, M. J. Ireland and S. Bernhard, *Chem. Eur. J.*, 2007, **13**, 8726.

29 P. Zhang, P. A. Jacques, M. Chavarot-Kerlidou, M. Wang, L. Sun, M. Fontecave and V. Artero, *Inorg. Chem.*, 2012, **51**, 2115.

30 (a) A. Reynal, E. Pastor, M. A. Gross, S. Selim, E. Reisner and J. R. Durrant, *Chem. Sci.*, 2015, **6**, 4855. (b) M. Natali, *ACS Catal.*, 2017, **7**, 1330.

31 A. Juris, V. Balzani, F. Barigelletti, S. Campagna, P. Belser and A. Von Zelewsky, *Coord. Chem. Rev.*, 1988, **84**, 85.

32 C. V. Krishnan and N. Sutin, *J. Am. Chem. Soc.*, 1981, **103**, 2141

33 (a) G. Tallec, D. Imbert, P. H. Fries and M. Mazzanti, *Dalton Trans.* 2010, **39**, 9490. (b) V. G. Ramsey, *J. Am. Pharm. Assoc.* 1951, **40**, 564. (c) L. Chen, C. Yan, B.-B. Du, K. Wu, L.-Y. Zhang, S.-Y. Yin and M. Pan, *Inorg. Chem. Commun.* 2014, **47**, 13.

34 K. J. Barnham, E. C. L. Gautier, G. B. Kok and G. Krippner, US20080161353 A1, 2008.

35 (a) M. S. Lowry, W. R. Hudson, R. A. Pascal Jr. and S. Bernhard, *J. Am. Chem. Soc.*, 2004, **126**, 14129. (b) I. Gonzáles, D. Cortés-Arriagada, P. Dreyse, L. Sanhueza-Vega, I. Ledoux-Rak, D. Andrade, I. Brito, A. Toro-Labbé, M. Soto-Arriaza, S. Caramori and B. Loeb, *Eur. J. Inorg. Chem.*, 2015, 4946.

View Article Online
DOI: 10.1039/C7DT02666H

TOC

Novel first-row transition metal complexes based on the 8-hydroxyquinoline-di(2-picolyl)amine ligand were prepared and tested as potential HECs in light-driven experiments.